J. Astron. Space Sci. 18(1), 15–20 (2001)

THE EVOLUTION OF AGB STARS ON INFRARED 2-COLOR DIAGRAMS

Kyung-Won Suh†, Jae Woo Lee and Hak-Youn Kim
Department of Astronomy and Space Science, Chungbuk National University
Cheongju, 361-763, Korea
E-mail: kwsuh@ast.chungbuk.ac.kr, jwlee@ast.chungbuk.ac.kr and kimhy@ast.chungbuk.ac.kr

(Received March 30, 2001; Accepted May 2, 2001)

ABSTRACT

We present infrared 2-color diagrams of AGB stars from the observations at near infrared and IRAS point source catalog (PSC) data. We compile the observations for thousands of newly identified OH/IR stars and carbon stars. We compare the observations with the theoretical evolutionary tracks of AGB stars. From the new observational data base and theoretical tracks, we discuss the meaning of the infrared 2-color diagrams.

Key words: AGB stars, dust, infrared

1. INTRODUCTION

Stars on the asymptotic giant branch (AGB) are generally classified into oxygen-rich stars (M-type Miras and OH/IR stars) and carbon-rich stars (carbon stars) based on photospheric abundance. van der Veen & Habing (1988, hereafter VH) used IRAS two-color diagram as a tool for studying late stages of stellar evolution. They divided the IRAS two-color diagram into eight areas which contain an astrophysically more or less homogeneous group. Epchtein et al. (1987, hereafter ELMP) used the $K - L$ color and the [12−25] color to distinguish carbon-rich stars from oxygen-rich stars. The two-color diagram provides a better discrimination of various types of objects than the IRAS two-color diagram. But, the two-color diagram was not useful at $K - L > 4$.

In this paper, we compare the theoretical evolutionary tracks with the observations of AGB stars. We compile the observations for thousands of newly classified OH/IR stars and carbon stars.

2. THEORETICAL MODELS

For this paper, we have used a numerical code developed by Ivezić & Elitzur (1997) that solves the radiative transfer spherical problem taking full advantage of scaling. We have performed the model calculations in the wavelength range 0.01 to 36000 μm.

For oxygen-rich stars, we use the optical constants of warm and cool silicate grains derived by Suh (1999). The radii of spherical dust grains have been assumed to be 0.1 μm uniformly. We

†corresponding author

choose 10 μm as the fiducial wavelength that sets the scale of the optical depth (τ_{10}) and compute models for various optical depths (τ_{10} = 0.01, 0.05, 0.1, 0.5, 3, 7, 15, 30 and 40). For the central star, we assume that the luminosity is 10^4 $L_\odot$ and a stellar blackbody temperature is 2500 K for τ_{10} $\leq$ 3 and 2000 K for $\tau_{10} > 3$. Also, we use the warm silicate dust grains for $\tau_{10} \leq 3$ and the cool ones for $\tau_{10} > 3$.

For carbon-rich stars, we use the optical constants of amorphous carbon (AMC) grains derived by Suh (2000) and the optical constants of α SiC grains by Pégourié (1988). The radii of spherical dust grains have been assumed to be 0.1 μm uniformly. We choose 10 μm as the fiducial wavelength that sets the scale of the optical depth (τ_{10}) and perform the model calculations for various optical depths ($\tau_{10} = 0.01, 0.1, 1, 2, 3$ and 5). For the central star, we assume that the luminosity is 10^4 $L_\odot$ and a stellar blackbody temperature is 2300 K for $\tau_{10} \leq 0.1$ and 2000 K for $\tau_{10} > 0.1$. For model of carbon-rich stars, we use simple mixture of AMC and SiC dust grains

For all the models, we assume the dust density distribution is inversely proportional to the square of the distance ($\rho \propto r^{-2}$). The dust condensation temperature (T_c) is assumed to be 1000 K and 500 K. The outer radius of the dust shell is always taken to be 10^4 times inner radius (R_c).

3. INFRARED 2-COLOR DIAGRAMS

Many investigators have classified the various types of AGB stars using various methods and techniques. We have collected the near infrared and IRAS PSC data of the identified stars as listed in Table 1. Figure 1 plots the oxygen- and carbon-rich stars in an IRAS two-color diagram using [12−25] versus [25−60], as well as the theoretical evolutionary tracks. The color index is defined by

$$M_{\lambda 1} - M_{\lambda 2} \quad = \quad 2.5 \log_{10} \frac{F_{\lambda 2}/ZMC_{\lambda 2}}{F_{\lambda 1}/ZMC_{\lambda 1}} \qquad (1)$$

where $ZMC_{\lambda i}$ means the zero magnitude calibration at given wavelength (λi). The magnitude scale is given in IRAS Explanatory Supplement (1987) (i.e., the zero magnitude fluxes at 12, 25, and 60 μm correspond to 28.3, 6.73 and 1.19 Jansky, respectively). Stars with good quality at any wavelength were used. The small symbols are the observational data and lines with large symbols are the models using the opacity functions for range in dust shell optical depth as we discussed in previous section.

In Figure 1, each box separates various areas that are more or less specific for astrophysically different objects. The boundary and stellar properties of each box were described by VH. As seen in Figure 1, the IRAS two-color diagram is not useful in discriminating between oxygen- and carbon-rich stars. So, we have collected the near-infrared observations to distinguish carbon-rich stars from oxygen-rich star and know the evolutionary track of AGB stars. We plot the $K - L$ versus [12−25] and $K-12$ versus [12−25] in Figure 2 and Figure 3, respectively. In Figure 2, the thick solid line is the boundary which separates between oxygen- and carbon-rich stars and the thick-dashed line corresponds to the spectral energy distributions of blackbody radiation. Oxygen-rich stars are distributed along T_c = 1000 K and 500 K. In Figure 2 and Figure 3, visual carbon stars lay in $K - L \leq 0.75$ and $K-12 \leq 1.7$ and silicate carbon stars lay in between infrared carbon stars and oxygen-rich stars.

In Figure 2, the boundary line derived by ELMP was not useful at $K - L > 4$. In this paper, we redefine the new boundary lines in the $K - L$ versus [12−25] and $K-12$ versus [12−25] to distinguish oxygen-rich stars from carbon-rich stars:

$$[12 - 25] = 1.0 + 0.15(K - L) \quad at\ K - L \geq 3.4 \qquad (2)$$

Table 1. The classified AGB stars as identified by many authors.

References	The number of the identified AGB stars				
	O[1]	J stars	Silicate C[2]	Visual C[2]	Infrared C[2]
Rowan-Robinson et al. (1986)	1				39
Chan & Kwok (1990)					145 (127,118)[3]
Epchtein et al. (1990)	21 (21,21)[3]				196 (196,194)[3]
Lewis et al. (1990)	86				
Egan & Leung (1991)				78 (77,75)[3]	47 (42,40)[3]
Le Squeren et al. (1992)	83				
Volk et al. (1992)					32 (19,16)[3]
Blommaert et al. (1993)	10				
Chan (1993)					69
Chengalur et al. (1993)	152				
David et al. (1993)	139				
Groenewegen et al. (1993)					25 (25,25)[3]
Guglielmo et al. (1993)					175 (175,175)[3]
Kastner et al. (1993)	18 (18,17)[3]				15 (15,14)[3]
Loup et al. (1993)	113				
Nyman et al. (1993)	41 (33,32)[3]				
van Loon et al. (1998)	12				
Volk et al. (1993)					6
Groenewegen et al. (1994)					5
Lorenz-Martins & Lefevre (1994)					2
Whitelock et al. (1994)	58 (58,58)[3]				3
Xiong et al. (1994)	58 (54,18)[3]				
Groenewegen (1995)					14
Groenewegen et al. (1995)					12
Lepine et al. (1995)	382 (357,336)[3]				
Guglielmo et al. (1997)	10 (10,10)[3]				20 (20,20)[3]
Kwok et al. (1997)		10 (10,10)[3]	9 (2,2)[3]	59 (45,36)[3]	
Lewis (1997)	229				
Willacy & Millar (1997)	4				
Guglielmo et al. (1998)	12 (12,12)[3]				27 (27,27)[3]
Chen et al. (1999)			3 (2,2)[3]		
Trams et al. (1999)			1 (1,1)[3]		
Jiang et al. (2000)			1		
Molster et al. (2001)		1 (1,1)[3]			
Total number	1429 (563,504)[3]	11 (11,11)[3]	14 (5,5)[3]	137 (122,111)[3]	832 (646,629)[3]

[1]: oxygen-rich stars
[2]: carbon-rich stars
[3]: the number of the stars observed at K and L bands, respectively

$$[12-25] = 0.4 + 0.13(K-12) \tag{3}$$

The lines are plotted as the thick solid line in Figure 2 and Figure 3. The "OS", "VCS" and "IRCS" represent oxygen-rich stars, visual carbon stars and infrared carbon stars, respectively.

4. CONCLUSIONS

In this paper, we have compiled the observations of AGB stars at near infrared and IRAS PSC data to understand their the evolutionary sequence. We have presented infrared 2-color diagrams of the stars and compared the observations with the theoretical evolutionary tracks in term of radiative

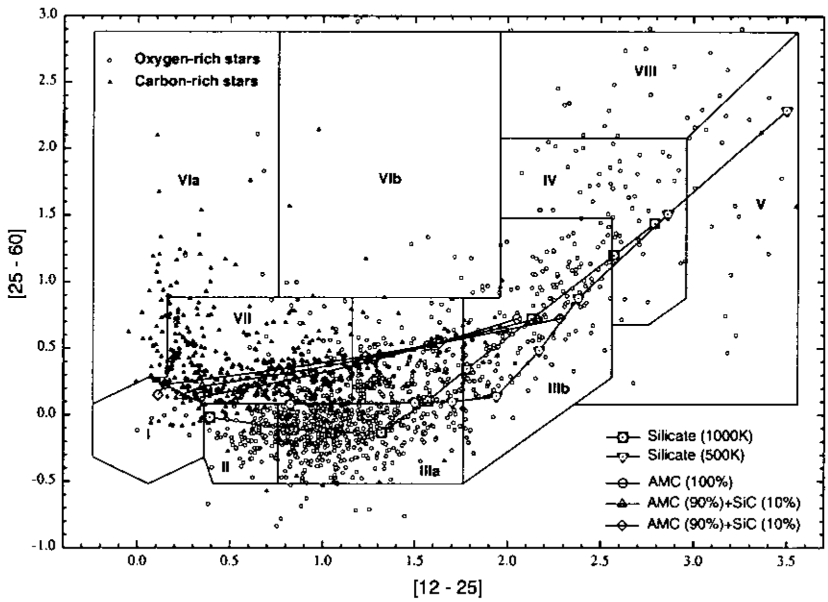

Figure 1. Loci of model results in the IRAS two-color diagram for oxygen- and carbon-rich AGB stars.

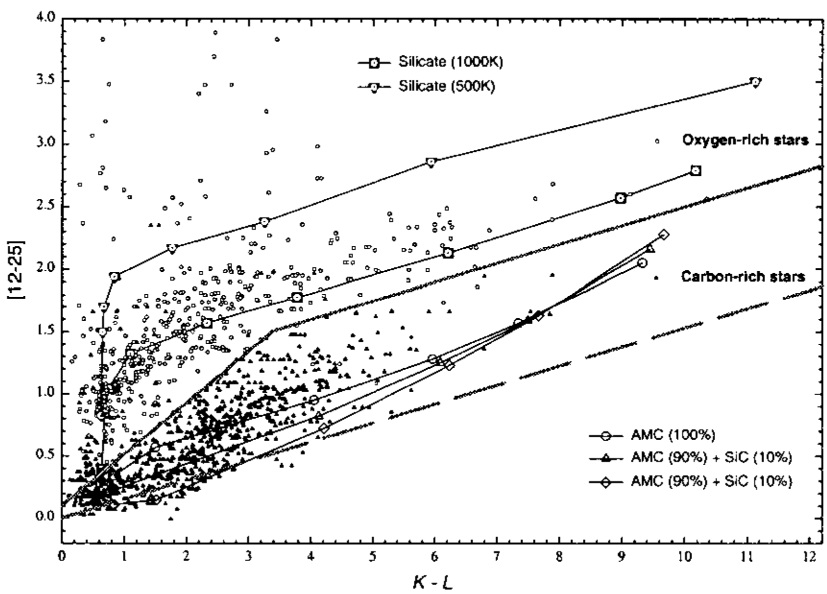

Figure 2. Loci of model results in the $K - L$ versus [12−25] for oxygen- and carbon-rich AGB stars.

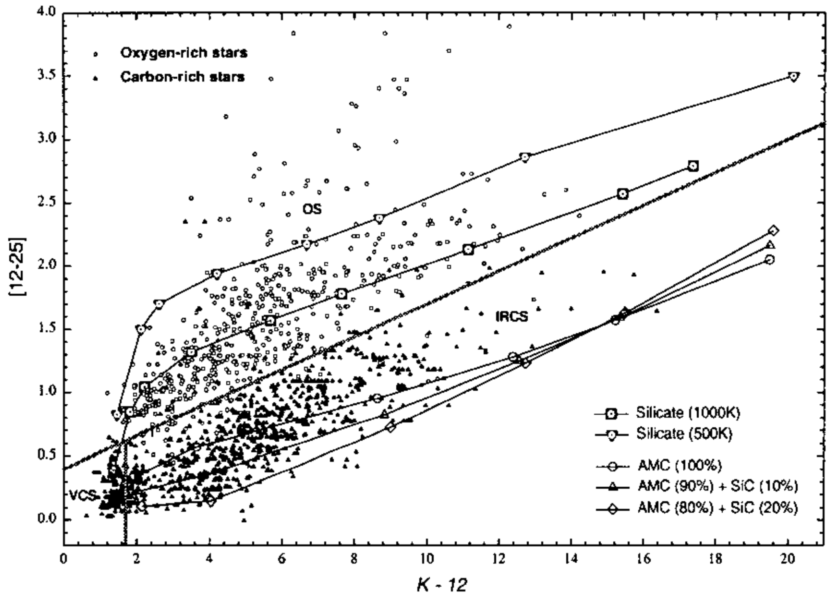

Figure 3. Loci of model results in the $K-12$ versus [12−25] for oxygen- and carbon-rich AGB stars. The "OS", "VCS" and "IRCS" represent oxygen-rich, visual carbon and infrared carbon stars, respectively.

transfer model results. In this paper, we have redefined the boundary lines in the 2-color diagrams to distinguish carbon-rich stars from oxygen-rich stars. The new separate lines cloud be useful for discriminating between oxygen-rich and carbon-rich AGB stars.

ACKNOWLEDGEMENTS: This work was supported by grant No. 2000-1-11300-001-3 from the Basic Research Program of the Korea Science & Engineering Foundation.

REFERENCES

Blommaert, J. A. D. L., van der Veen, W. E. C. J., & Habing, H. J. 1993, A&A, 267, 39

Chan, S. J. 1993, PASP, 105, 1107

Chan, S. J., & Kwok, S. 1990, A&A, 237, 354

Chen, P. -S., Wang, X. -H., & Wang, F. 1999, Acta Astron. Sinica, 40, 32

Chengalur, J. N., Lewis B. M., Eder, J., & Terzian, Y. 1993, ApJS, 89, 189

David, P., Le Squeren, A. M., & Sivagnanam, P. 1993, A&A, 277, 453

Egan, M. P., & Leung, C. M. 1991, ApJ, 383, 314

Epchtein, N., Le Bertre, T., & Lepine, J. R. D. 1990, A&A, 227, 82

Epchtein, N., Le Bertre, T., Lepine, J. R. D., Marques dos Santos, P., Matsuura, O. T., & picazzio, E. 1987, A&AS, 71, 39 (ELMP)

Groenewegen, M. A. T. 1995, A&A, 293, 463

Groenewegen, M. A. T., de Jong, T., & Baas, F. 1993, A&AS, 101, 513

Groenewegen, M. A. T., de Jong T., & Geballe, T. R. 1994, A&A, 287, 163

Groenewegen, M. A. T., van den Hoek, L. B., & de Jong T. 1995, A&A, 293, 381
Guglielmo, F., Epchtein, N., Arditti, F., & Sevre, F. 1997, A&AS, 122, 489
Guglielmo, F., Epchtein, N., Le Bertre, T., Fouque, P., Hron, J., Kerschbaum, F., & Lepine, J. R. D. 1993, A&AS, 99, 31
Guglielmo, F., Le Bertre, T., & Epchtein, N. 1998, A&A, 334, 609
IRAS Science Team, 1987, Catalogs and Atlases
Ivezić, A., & Elitzur, M. 1997, MNRAS, 287, 799
Jiang, B. W., Szczerba, R., & Deguchi, S. 2000, A&A, 362, 273
Kastner, J. H., Forveille, T., Zuckerman, B., & Omont, A. 1993, A&A, 275, 163
Kwok, S., Volk, K., & Bidelman, W. P. 1997, ApJS, 112, 557
Le Squeren, A. M., Sivagnanam, P., Dennefeld, M., & David, P. 1992, A&A, 254, 133
Lepine, J. R. G., Ortiz, R., & Epchtein, N. 1995, A&A, 299, 453
Lewis, B. M. 1997, ApJ, 109, 489
Lewis, B. M., Eder, J., & Terzian, Y. 1990, ApJ, 362, 634
Lorenz-Martins, S., & Lefevre, J. 1994, A&A, 291, 831
Loup, C., Forveille, T., Omont, A., & Paul, J. F. 1993, A&AS, 99, 291
Molster, F. J., Yamamura, I., Waters, L. B. F. M., Nyman, L. -A., Käufl, H. -U., de Jong, T., & Loup, C. 2001, A&A, 366, 923
Nyman, L.-A., Hall, P. J., & Le Bertre, T. 1993, A&A, 280, 551
Pégourié, B. 1988, A&A, 194, 335
Rowan-Robinson, M., Lock, T. D., Walker, D. W., & Harris, S. 1986, MNRAS, 222, 273
Suh, K.-W. 1999, MNRAS, 304, 389
Suh, K.-W. 2000, MNRAS, 315, 740
Trams, N. R., van Loon, J. Th., Zijlstra, A. A., Loup, C., Groenewegen, M. A. T., Waters, L. B. F. M., Whitelock, P. A., Blommaert, J. A. D. L., Siebenmorgen, R., & Heske, A. 1999, A&A, 344, 17
van der Veen, W. E. C. J., & Habing, H. J. 1988, A&A, 194, 125 (VH)
van Loon, J. Th., Zijlstra, A. A., Whitelock, P. A., Hekkert, P. L., Chapman, J. M., Loup, C., Groenewegen, M. A. T., Waters, L. B. F. M., & Trams, N. R. 1998, A&A, 329, 169
Volk, K., Kwok, S., & Langill, P. P. 1992, ApJ, 391, 285
Volk, K., Kwok, S., & Woodsworth, A. W. 1993, ApJ, 402, 292
Whitelock, P., Menzies, J., Michael, F., Marang, F., Carter, B., Roberts, G., Catchpole, R., & Chapman, J. 1994, MNRAS, 267, 711
Willacy, K., & Millar, T. J. 1997, A&A, 324, 237
Xiong, G. Z., Chen, P. S., & Gao, H. 1994, A&AS, 108, 661